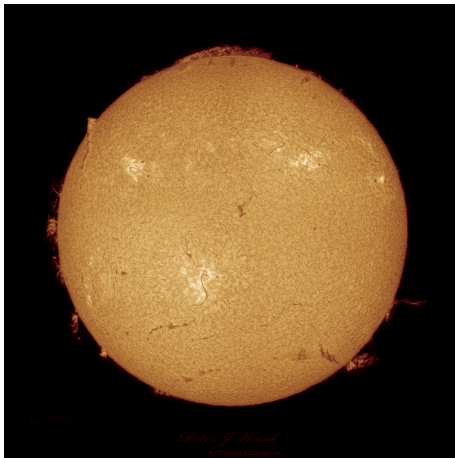


# Modélisation d'un écoulement en convection stratifié: des équations anélastiques aux simulations numériques

Mouloud Kessar

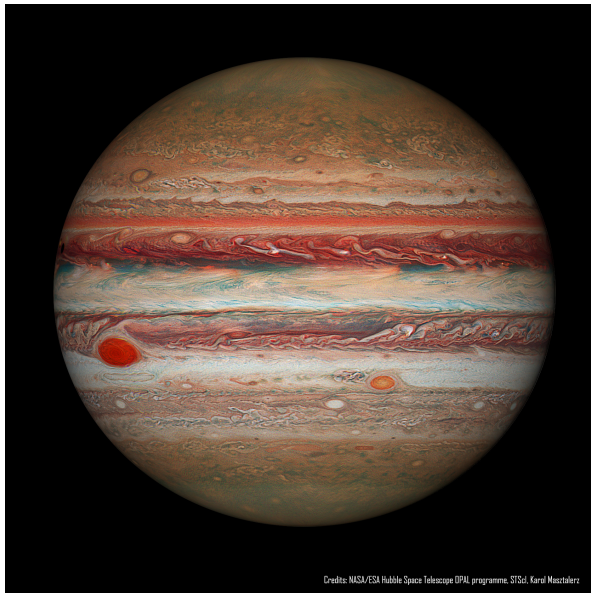
03/02/2023

# La zone de convection du Soleil

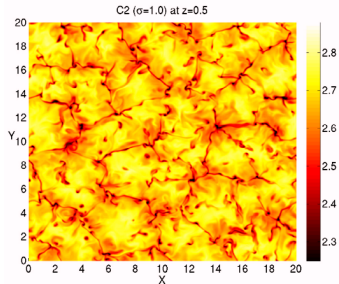
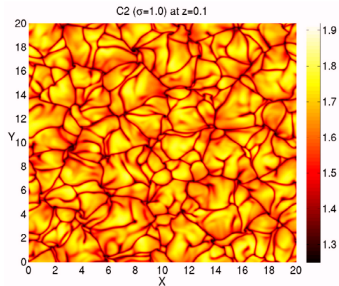
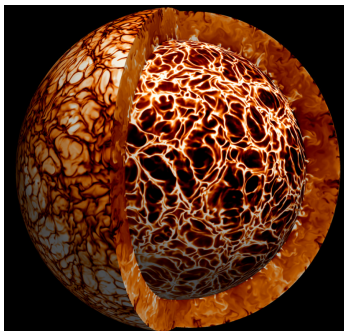


rapport de densité de l'ordre de  $10^6$  à travers la zone de convection

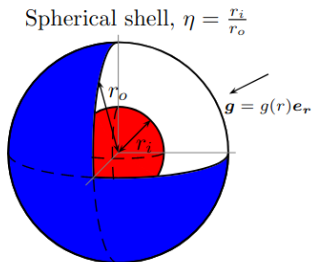
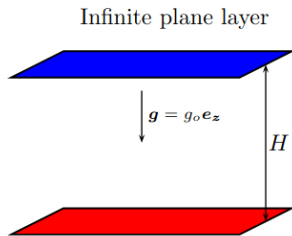
# l'atmosphère de Jupiter



# Simulations à 3D: Globales ou locales



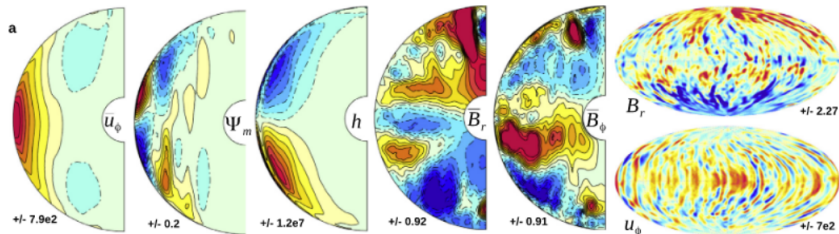
# Simulations à 3D: Globales ou locales



- Conditions aux limites Stress free: modélisation d'étoiles et de géantes gazeuses.
- Conditions aux limites No-Slip: modélisation du coeur de planètes telluriques.

- La présence d'ondes sonores: impose de trop petits pas de temps
- l'approximation anélastique:  $\operatorname{div}(\rho\mathbf{u}) = 0$
- 2014: Il n'existe pas de code local,3D, de magnéto-convection anélastique
  
- 2015: Début du développement d'un code de convection anélastique à 3D en géométrie cartésienne

- I Une approximation anélastique
- II Une méthode numérique
- III Une structure de code
- IV Amélioration des performances du code
- V Amélioration du choix des algorithmes: le cas du CNAB2
- VI Résultats du code



- Code Anélastique développé par Ashley Willis.
- Sert d'inspiration sur le model et la méthode numérique pour développer un code cartésien.

$$\frac{\partial \mathbf{u}}{\partial t} + (\mathbf{u} \cdot \nabla) \mathbf{u} = -\nabla \left( \frac{p}{\bar{\rho}} \right) + \mathcal{R} \sigma_m \sigma_\eta^{-1} s \hat{\mathbf{e}}_z - T^{1/2} \sigma_m \hat{\mathbf{e}}_z \times \mathbf{u} + \frac{M^2 \sigma_m}{\bar{\rho}} (\nabla \times \mathbf{B}) \times \mathbf{B} + \frac{\sigma_m}{\bar{\rho}} \left[ \nabla^2 \mathbf{u} + \frac{1}{3} \nabla (\nabla \cdot \mathbf{u}) \right]$$

$$\frac{\partial \mathbf{B}}{\partial t} = \nabla \times (\mathbf{u} \times \mathbf{B}) + \nabla^2 \mathbf{B}$$

$$\nabla \cdot (\bar{\rho} \mathbf{u}) = 0$$

$$\nabla \cdot \mathbf{B} = 0$$

$$\begin{aligned} \frac{\partial s}{\partial t} + \mathbf{u} \cdot \nabla s - \frac{u_z}{1 + \theta z} &= \frac{\sigma_\eta^{-1}}{\bar{\rho}} \nabla^2 s + \frac{\sigma_\eta^{-1} \theta}{\bar{\rho} \bar{T}} \frac{\partial s}{\partial z} - \frac{\theta M^2 \sigma_\eta}{\mathcal{R}} \frac{1}{\bar{\rho} \bar{T}} (\nabla \times \mathbf{B})^2 + \\ &- \frac{\theta \sigma_\eta}{\mathcal{R}} \frac{1}{\bar{\rho} \bar{T}} \left[ 2 \sum_{i=1}^3 \left( \frac{\partial u_i}{\partial x_i} \right)^2 + \sum_{i < j} \left( \frac{\partial u_i}{\partial x_j} + \frac{\partial u_j}{\partial x_i} \right)^2 - \frac{2}{3} (\nabla \cdot \mathbf{u})^2 \right] \end{aligned}$$

- d'après Lantz & Fan (1999)

$$\bar{\rho}\mathbf{u} = \nabla \times (\bar{\rho}\mathcal{T}_u \hat{\mathbf{e}}_z) + \nabla \times \nabla \times (\bar{\rho}\tilde{\mathcal{P}}_u \hat{\mathbf{e}}_z) + \bar{\rho}\langle \mathbf{u} \rangle_h \equiv \bar{\rho}\mathbf{u}' + \bar{\rho}\langle \mathbf{u} \rangle_h$$

$$\text{Let: } \mathcal{P}_u \equiv \bar{\rho}\tilde{\mathcal{P}}_u$$

$$\mathbf{B} = \nabla \times (\mathcal{T}_B \hat{\mathbf{e}}_z) + \nabla \times \nabla \times (\mathcal{P}_B \hat{\mathbf{e}}_z) + \langle \mathbf{B} \rangle_h = \mathbf{B}' + \langle \mathbf{B} \rangle_h$$

$$\frac{\partial \langle u_x \rangle_h}{\partial t} = -\langle \mathbf{u} \cdot \nabla u_x \rangle_h + M^2 \sigma_m \frac{1}{\bar{\rho}} \langle \mathbf{B} \cdot \nabla B_x \rangle_h + T^{1/2} \sigma_m \langle u_y \rangle_h + \frac{\sigma_m}{\bar{\rho}} \frac{\partial^2 \langle u_x \rangle_h}{\partial z^2}$$

$$\frac{\partial \langle u_y \rangle_h}{\partial t} = -\langle \mathbf{u} \cdot \nabla u_y \rangle_h + M^2 \sigma_m \frac{1}{\bar{\rho}} \langle \mathbf{B} \cdot \nabla B_y \rangle_h - T^{1/2} \sigma_m \langle u_x \rangle_h + \frac{\sigma_m}{\bar{\rho}} \frac{\partial^2 \langle u_y \rangle_h}{\partial z^2}$$

$$\frac{\partial \langle B_x \rangle_h}{\partial t} = -\frac{\partial}{\partial z} \langle u_z B_x - u_x B_z \rangle_h + \frac{\partial^2 \langle B_x \rangle_h}{\partial z^2}$$

$$\frac{\partial \langle B_y \rangle_h}{\partial t} = \frac{\partial}{\partial z} \langle u_y B_z - u_z B_y \rangle_h + \frac{\partial^2 \langle B_y \rangle_h}{\partial z^2}$$

# Equation poloidale et toroidale

for  $k_x \neq 0$  or  $k_y \neq 0$  :

$$\frac{\partial}{\partial t} \mathfrak{D}^2 \hat{P}_u = -\frac{i}{k^2} \left( k_x \frac{\partial \hat{\mathcal{X}}}{\partial z} + k_y \frac{\partial \hat{\mathcal{Y}}}{\partial z} \right) - \hat{Z} - \mathcal{R} \sigma_m \sigma_\eta^{-1} \hat{s} - \sigma_m T^{1/2} \frac{\partial \hat{T}_u}{\partial z} + \frac{4}{3} \frac{\sigma_m m^2 \theta^2}{\bar{\rho}^2 \bar{T}^2} k^2 \hat{P}_u + \sigma_m \mathfrak{D}^2 \mathfrak{D}^2 \hat{P}_u$$

$$\mathfrak{D}^2 = \frac{1}{\bar{\rho}} \nabla^2 - \frac{m\theta}{\bar{\rho} \bar{T}} \frac{\partial}{\partial z}$$

$$\frac{\partial \hat{T}_u}{\partial t} = \frac{i}{k^2} [k_x \hat{\mathcal{Y}} - k_y \hat{\mathcal{X}}] + \frac{\sigma_m T^{1/2}}{\bar{\rho}} \frac{\partial \hat{P}_u}{\partial z} + \frac{\sigma_m}{\bar{\rho}} \left( -k^2 + \frac{\partial^2}{\partial z^2} \right) \hat{T}_u$$

$$\frac{\partial \hat{T}_B}{\partial t} = \hat{G}_z + \frac{i}{k^2} \frac{\partial}{\partial z} (k_x \hat{G}_x + k_y \hat{G}_y) + \left( -k^2 + \frac{\partial^2}{\partial z^2} \right) \hat{T}_B$$

$$\frac{\partial \hat{P}_B}{\partial t} = \frac{i}{k^2} (k_x \hat{G}_y - k_y \hat{G}_x) + \left( -k^2 + \frac{\partial^2}{\partial z^2} \right) \hat{P}_B$$

$$\frac{\partial \hat{s}}{\partial t} = -\widehat{\mathbf{u} \cdot \nabla} s + \frac{k^2}{\bar{\rho} \bar{T}} \hat{P}_u + \frac{\sigma_\eta^{-1}}{\bar{\rho}} \left( -k^2 + \frac{\partial^2}{\partial z^2} + \frac{\theta}{\bar{T}} \frac{\partial}{\partial z} \right) \hat{s} - \frac{\theta \sigma_\eta M^2}{\mathcal{R}} \frac{1}{\bar{\rho} \bar{T}} \hat{J}_h - \frac{\theta \sigma_\eta}{\mathcal{R}} \frac{1}{\bar{\rho} \bar{T}} \hat{V}_h$$

$$\mathbf{u} = \begin{bmatrix} \partial_y \mathcal{I}_u + \bar{\varrho}^{-1} \partial_x \partial_z \mathcal{P}_u \\ -\partial_x \mathcal{I}_u + \bar{\varrho}^{-1} \partial_y \partial_z \mathcal{P}_u \\ -\bar{\varrho}^{-1} \nabla_h^2 \mathcal{P}_u \end{bmatrix} + \begin{bmatrix} \langle u_x \rangle_h \\ \langle u_y \rangle_h \\ 0 \end{bmatrix}$$

$$\hat{\mathcal{I}}_u = \frac{i}{k^2} (k_x \hat{u}'_y - k_y \hat{u}'_x)$$

$$\hat{\mathcal{P}}_u = \frac{\bar{\varrho}}{k^2} \hat{u}'_z$$

$$\mathbf{B} = \begin{bmatrix} \partial_y \mathcal{I}_B + \partial_x \partial_z \mathcal{P}_B \\ -\partial_x \mathcal{I}_B + \partial_y \partial_z \mathcal{P}_B \\ -\nabla_h^2 \mathcal{P}_B \end{bmatrix} + \begin{bmatrix} \langle B_x \rangle_h \\ \langle B_y \rangle_h \\ \mathfrak{B} \end{bmatrix}$$

$$\hat{\mathcal{I}}_B = \frac{i}{k^2} (k_x \hat{B}'_y - k_y \hat{B}'_x)$$

$$\hat{\mathcal{P}}_B = \frac{1}{k^2} \hat{B}'_z$$

# Le problème de l'équation Poloidale

$$\frac{\partial}{\partial t} \mathfrak{D}^2 \hat{\mathcal{P}}_u = \hat{\mathfrak{R}} + \sigma_m \mathfrak{D}^2 \mathfrak{D}^2 \hat{\mathcal{P}}_u$$

where

$$\hat{\mathfrak{R}} = -\frac{i}{k^2} \left( k_x \frac{\partial \hat{\mathcal{X}}}{\partial z} + k_y \frac{\partial \hat{\mathcal{Y}}}{\partial z} \right) - \hat{\mathcal{Z}} - \mathcal{R} \sigma_m \sigma_{\eta}^{-1} \hat{s} - \sigma_m T^{1/2} \frac{\partial \hat{\mathcal{T}}_u}{\partial z} + \frac{4 \sigma_m m^2 \theta^2}{3 \bar{\varrho}^2 T^2} k^2 \hat{\mathcal{P}}_u \quad \text{and} \quad \mathfrak{D}^2 = \frac{1}{\bar{\varrho}} \nabla^2 - \frac{m\theta}{\bar{\varrho} T} \frac{\partial}{\partial z}$$

and it is subject to either no-slip  $\left( \hat{\mathcal{P}}_u|_{z=0,1} = 0, \partial_z \hat{\mathcal{P}}_u|_{z=0,1} = 0 \right)$  or stress-free  $\left( \hat{\mathcal{P}}_u|_{z=0,1} = 0, \mathfrak{D}^2 \hat{\mathcal{P}}_u|_{z=0,1} = 0 \right)$  boundary conditions, where  $\mathfrak{D}^2 = \partial_z^2 - \frac{m\theta}{T} \partial_z$ . Hence defining the following operator

$$\mathcal{O}_t = \partial_t - \sigma_m \mathfrak{D}^2$$

time-dependent problem (solved at every time-step for different  $\hat{\mathfrak{R}}(t)$ )

$$\begin{cases} \mathcal{O}_t \hat{\mathcal{P}}_u^{(0)} = \hat{\Lambda}^{(0)} \\ \mathfrak{D}^2 \hat{\Lambda}^{(0)} = \hat{\mathfrak{R}}(t) \end{cases} \quad \text{with} \quad \left( \partial_z \hat{\mathcal{P}}_u^{(0)} \Big|_{z=0,1} = 0 \quad \text{or} \quad \mathfrak{D}^2 \hat{\mathcal{P}}_u^{(0)} \Big|_{z=0,1} = 0 \right) \quad \text{and} \quad \hat{\Lambda}^{(0)} \Big|_{z=0,1} = 0$$

two independent of time sets of equations for Green's functions, which can be found in preprocessing:

$$\begin{cases} \mathcal{O}_t \hat{G}_{\mathcal{P}_u}^{(1)} = \hat{\Lambda}^{(1)} \\ \mathfrak{D}^2 \hat{\Lambda}^{(1)} = 0 \end{cases} \quad \text{with} \quad \left( \partial_z \hat{G}_{\mathcal{P}_u}^{(1)} \Big|_{z=0,1} = 0 \quad \text{or} \quad \mathfrak{D}^2 \hat{G}_{\mathcal{P}_u}^{(1)} \Big|_{z=0,1} = 0 \right) \quad \text{and} \quad \left( \hat{\Lambda}^{(1)} \Big|_{z=0} = 1, \quad \hat{\Lambda}^{(1)} \Big|_{z=1} = 0 \right)$$

$$\begin{cases} \mathcal{O}_t \hat{G}_{\mathcal{P}_u}^{(2)} = \hat{\Lambda}^{(2)} \\ \mathfrak{D}^2 \hat{\Lambda}^{(2)} = 0 \end{cases} \quad \text{with} \quad \left( \partial_z \hat{G}_{\mathcal{P}_u}^{(2)} \Big|_{z=0,1} = 0 \quad \text{or} \quad \mathfrak{D}^2 \hat{G}_{\mathcal{P}_u}^{(2)} \Big|_{z=0,1} = 0 \right) \quad \text{and} \quad \left( \hat{\Lambda}^{(2)} \Big|_{z=0} = 0, \quad \hat{\Lambda}^{(2)} \Big|_{z=1} = 1 \right)$$

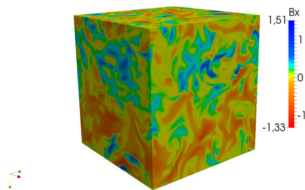
Thus the solution at time  $t$  (satisfying all the boundary conditions) is given by:

$$\hat{\mathcal{P}}_u(t) = \hat{\mathcal{P}}_u^{(0)}(t) + a \hat{G}_{\mathcal{P}_u}^{(1)} + b \hat{G}_{\mathcal{P}_u}^{(2)}$$

where the constants  $a$  and  $b$  are found by imposing  $\hat{\mathcal{P}}_u(t) \Big|_{z=0,1} = 0$ , hence

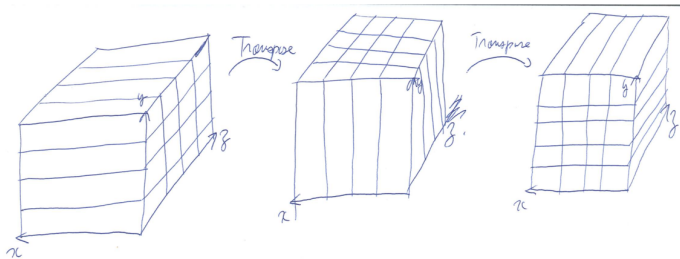
## Numerical tool: code SCALES

- Pseudo-spectral code developed at LEGI
- HD, MHD, passive scalar transport
- DNS, LES
- FFTW
- HDF5
- MPI



Visualization of the magnetic field

# Parallélisation



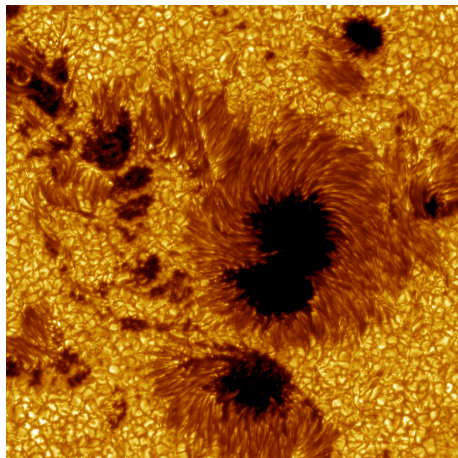
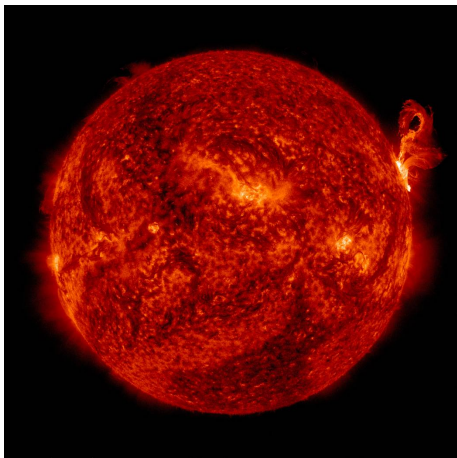
# Types dérivées

```
1336     do q=Dyux_r%zmin, Dyux_r%zmax
1337     do i=Dyux_r%xmin, Dyux_r%xmax
1338     do j=Dyux_r%ymmin, Dyux_r%ymax
1339
1340         J_H%values(i, j, q) = -(theta*Sigma_eta*HartMann**2.0_8/(RA*density(q)*Temperature(q)))*&
1341             & ( ( DxB_y_r%values(i, j, q) - DyB_x_r%values(i, j, q) )**2.0_8 &
1342             & + ( DyB_z_r%values(i, j, q) - DzB_y_r%values(i, j, q) )**2.0_8 &
1343             & + ( DzB_x_r%values(i, j, q) - DxB_z_r%values(i, j, q) )**2.0_8 )
1344
1345     enddo
1346 enddo
1347 enddo
1348
1349 ! endif
1350
1351 call forward_transform(J_H, J_HK, rank, res)
1352
1353 do q= NLT_entropy%czmin, NLT_entropy%czmax
1354     do ky = NLT_entropy%cymin, NLT_entropy%cymax
1355     do kx = NLT_entropy%cxmin, NLT_entropy%cxmax
1356         NLT_entropy%values(kx, ky, q) = NLT_entropy%values(kx, ky, q) + J_HK%values(kx, ky, q)
1357
1358     enddo
1359 enddo
1360 enddo
```

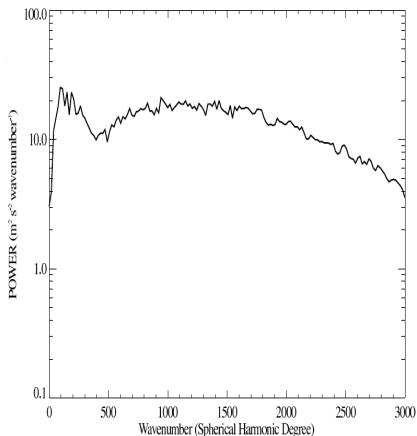
- intégrateur IMEX: CNAB2  $dt=cst$
- entrée sorties: HDF5

- 20% du temps dans MPI
- Supprimer lapack et remplacer par un pivot avec communication point a point pour supprimer 1 transposition par FFT
- Beaucoup de temps perdu dans le calcul des différences finies

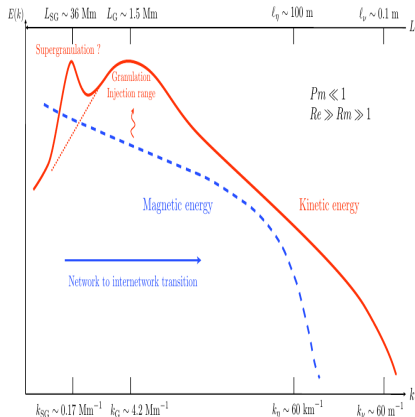
# Observations (I)



# Observations (II)

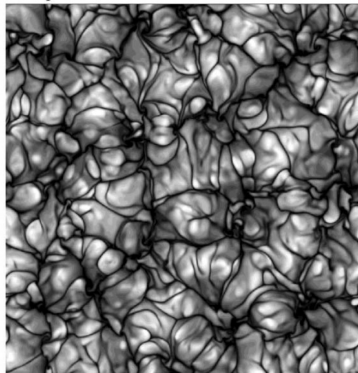


Power spectra of the Sun from Hathaway et al (2000).

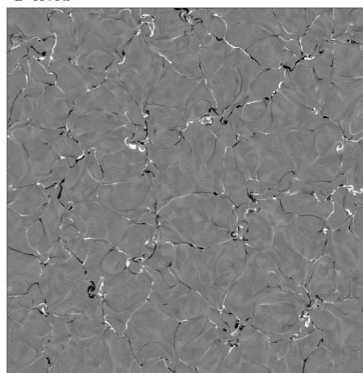


Schematic representation of the power spectra of the Sun from Rieutord & Rincon (2010).

# Numerics (I)



Horizontal slice of a Temperature field from Cattaneo(1999).



Horizontal slice of The vertical Magnetic field from Cattaneo(1999).

Granules have a large range of different sizes, but the vertical components of the magnetic field and vorticity are more intense between the

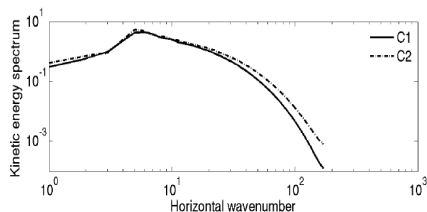
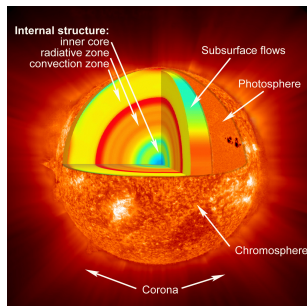


**Figure:** Kinetic energy spectrum from (Bushby & Favier, 2014)

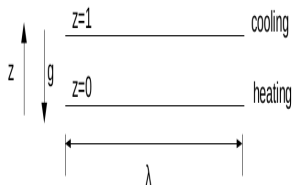
- "Mesogranules" are associated to the most energetic scale of the flow.
- Recent work (Bushby & Favier, 2014) showed this mesoscales were enhancing the dynamo action.



## Problematic

- Most of numerical studies on "mesogranules" have been performed for small density contrasts.
- What would happen to mesogranules if we were to increase the stratification?
- Is there a depth dependency on the size of mesogranules?

# Anelastic Approximation



## Reference state

$$\bar{T} = 1 + \theta z$$

$$\bar{\rho} = (1 + \theta z)^m$$

$$\bar{s} = c_v \ln \frac{p}{\bar{\rho}^\gamma}$$

$\mu$  and  $k$  are chosen

$$\partial_t \mathbf{u} + (\mathbf{u} \cdot \nabla) \mathbf{u} = \nabla P + R_a P_r s \mathbf{e}_z + \frac{P_r}{\bar{\rho}} \left[ \nabla^2 u + \frac{1}{3} \nabla(\nabla \cdot \mathbf{u}) \right]$$

$$\partial_t s + \mathbf{u} \cdot \nabla s = \frac{u_z}{\bar{T}} + \frac{1}{\bar{\rho}} \left[ \nabla^2 s + \frac{\theta}{\bar{T}} \frac{\partial s}{\partial z} \right]$$

$$- \frac{\theta}{R_a \bar{T} \bar{\rho}} \left[ 2 \sum_{i=1}^3 \left( \frac{\partial u_i}{\partial x_i} \right)^2 + \frac{2}{3} (\nabla \cdot \mathbf{u})^2 + \sum_{i < j}^3 \left( \frac{\partial u_i}{\partial x_j} + \frac{\partial u_j}{\partial x_i} \right)^2 \right]$$

$$\nabla \cdot (\bar{\rho} \mathbf{u}) = 0$$

- 3D cartesian code (can also do 2D)
- periodic boundary conditions in  $x$  and  $y$
- Stress Free or Non-slip in  $z$ ( velocity)
- Fixed entropy
- Fourier in  $x$  and  $y$ / finite differences in  $z$
- semi-implicit multi-stepping: Adams-Bashforth (2nd order) and Crank-Nicolson
- CODE resorts to MPI/FFTW/HDF5/LAPACK

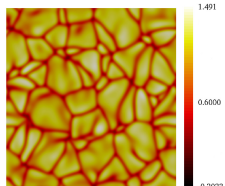
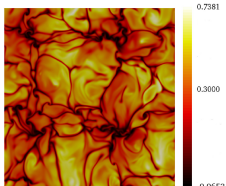
# Study's method

	BC	AC4	AC30	AC50
$\theta$	0	-0.60	-0.89	-0.92
$\rho_b/\rho_t$	1	4	30	50
$R_a$	$0.5 \times 10^6$	$1.2 \times 10^6$	$2.65 \times 10^6$	$2.95 \times 10^6$
$P_r$	1	1	1	1
$\lambda$	10	10	10	10
<i>Gridpoints</i>	$512^2 \times 128$	$512^2 \times 128$	$512^2 \times 256$	$512^3$

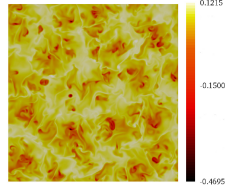
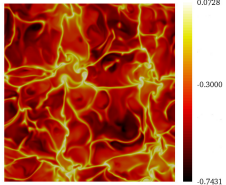
We start from a Boussinesq configuration ( Cattaneo 1999). And increase the density contrast whilst keeping  $Ra/Ra_c = cst$

# Entropy fluctuations

$z =$   
0.9



$z =$   
0.1



Temperature BC

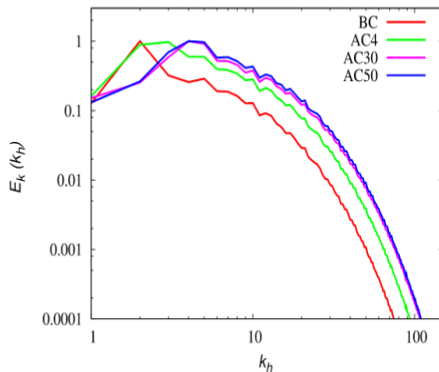
Entropy AC50

AC50

Turbulence is absent near the surface: we observe a range of convective cells

Turbulence is very strong close to the bottom : it is hard to see convective

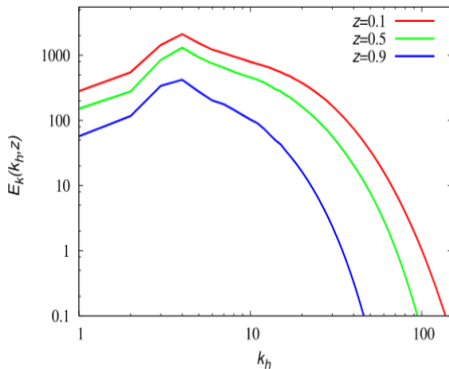
# Kinetic energy spectrum (I)



Depth and time averaged spectrum

Some configurations show a pic at smaller scales, but no clear trend

# Kinetic energy spectrum(II)



## Depth dependence (AC50)

The Most energetic scale is the same at every depth

More energy in the small scales at the bottom: turbulence is stronger inside the Sun.

## Summary

Increasing the stratification leads to a turbulence being much stronger at the bottom than at the top

This size of this convective scale remains the same at all depth